A COMPUTATIONAL STUDY OF SUBSONIC FLOWFIELDS OVER A MISSILE CONFIGURATION

I.H.Tuncer,* M.F. Platzer†
Department of Aeronautics and Astronautics
Naval Postgraduate School, Monterey, California
R.D. VanDyken‡
Naval Air Warfare Center Weapons Division, China Lake, CA

ABSTRACT

Subsonic flowfields over a missile configuration are computed at high angles of attack ranging from 15° to 60° using the NASA-Ames OVERFLOW Navier-Stokes solver. The computed flowfields are presented in terms of particle traces, helicity contours and surface streamlines. The flow separation over the missile body, development of leeward side vortex patterns, canard and tail vortices and their interaction are identified. The computed normal force and pitching moment coefficients compare well with the experimental data at 15° incidence. At the higher incidences the normal force is underpredicted by up to 15 percent. The computed pitching moments agree qualitatively well with the experimental data, but percentage deviations are substantial in the higher incidence range.

INTRODUCTION

The flow over a full missile configuration with canards and tails at high angles of attack is highly complex due to flow separation, formation of canard and body vortices and their interaction. Studying the complex flowfield and understanding the effect of the canards on the performance, stability characteristics and development of flow asymmetries are crucial to efforts in designing future missile airframes. The present work is aimed at utilizing the current CFD methods for investigating the complex flowfields and validating the computed results with experimental data.

Investigations on the aerodynamic characteristics of canard-controlled missiles at high angles of attack is of considerable interest because future combat aircraft may have the capability to maintain controlled flight at low speeds and high incidence angles. Therefore, in this flight regime missiles may be launched at a large angle of attack compared to traditional launches at angles of attack of no more than 10° to 15°. The resulting high angle of attack flowfield over a missile is vortex dominated with vortex breakdown and asymmetric vortex flow behavior, which lead to unpredictable aerodynamic forces and pose a potential threat to flight stability. Thus, a better understanding of the missile aerodynamics at high angles of attack is needed to expand missile launch windows and to improve future missile designs.

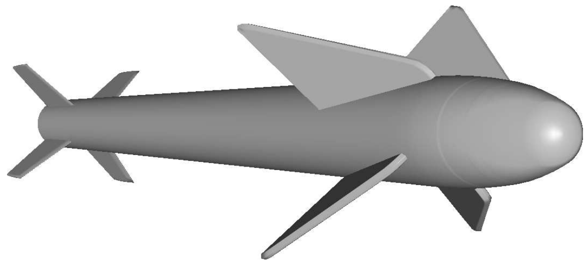

Fig. 1 Missile configuration at 10° canard deflection.

The current design tools for missile airframes range from semi-empirical methods to Navier-Stokes solvers[1,2]. A recent comprehensive review of high angle of attack aerodynamics has been given by Rom[1]. Recent Navier-Stokes computations[3,4,5,6,7] of flowfields around complete aircraft and missile configurations at high angles of attack show encouraging agreement with available experimental data. Schiff et al. [3,4] studied flows over a slender ogive-cylinder body of revolution at high angles of attack by solving the thin-layer Navier-Stokes equations. They calculated the growth of cross-flow separation and the development of leeward side vortex patterns, and identified the unsteadiness of the flowfields at high angles of attack.

Recently, Ekaterinaris[5] and Hsieh et al.[6] studied a full missile configuration at low subsonic speeds and high angles of attack. Hsieh employed the GASP Navier-Stokes

*Research Assistant Professor, Member AIAA
†Professor, Associate Fellow AIAA
‡Member AIAA

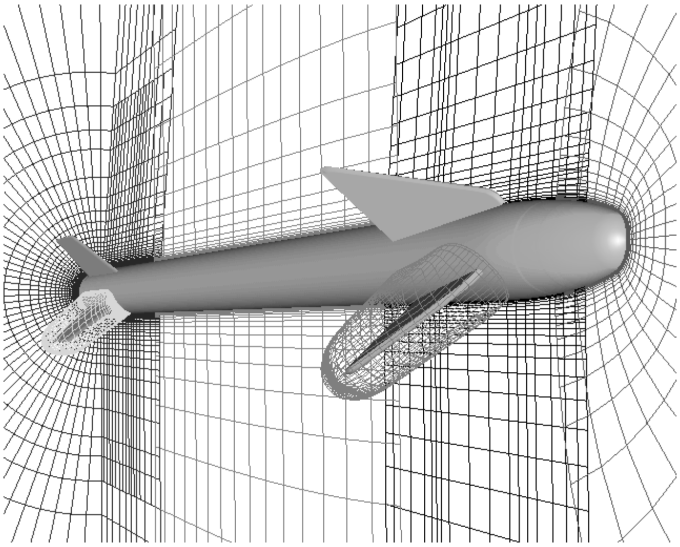

Fig. 2 Overset computational grid (Every other grid point is plotted)

solver to compute laminar flows over the missile at 0° roll angle (+ configuration), 0° canard deflection and 15, 30, 45, and 60° angles of attack. Ekaterinaris[5] computed the turbulent flow over the same missile configuration at 45° roll angle (X configuration) and 45° angle of attack. These computations were found to be in good agreement with the experimental force and moment data obtained by Smith et al[8]. in the Naval Postgraduate School wind tunnel and by Smith and Smith[9] in the NASA-Ames $7' \times 10'$ wind tunnel.

In this work, we build upon the work done by Ekaterinaris[5]. Subsonic flowfields around the missile configuration (Figure 1) are computed using the OVERFLOW thin layer Navier-Stokes solver. The computed flowfields between 15° and 60° are analyzed in terms of particles traces and surface streamlines. The integrated aerodynamic loads are compared against the experimental data of Smith and Smith[9].

NUMERICAL METHOD

Figure 1 shows the missile configuration studied. The missile is of 22.6 diameters in length. It has 67° swept delta canards with a root chord length of 2.5 diameters and 45° swept trapezoidal tails with a root chord length of 3 diameters. The tails are attached to the missile body and positioned parallel to the missile axis. Whereas the canards are separated from the body by a small gap, and can be set at a prescribed canard deflection, δ. The gap between the canard and the body, which becomes more distinguished when the canards are set at an angle, is taken into consideration during the discretization of the computational domain.

The same missile configuration was also employed in an experimental study conducted by Smith and Smith[9]. In the experiments a one-third-scale model was sting-mounted on a precision balance. The presence of the sting was also taken into consideration in the present computations.

The OVERFLOW Navier-Stokes solver (Version 1.6ao), developed at NASA-Ames[10,11] is employed to solve viscous flowfields over the missile configuration. The computational domain, which consists of the missile body, the sting, the canards and the tails, and the flowfield around them, is partitioned into zonal blocks. The zonal blocks are discretized with structured subgrids, which are overset onto each other. The OVERFLOW solver computes flowfields in each subgrid implicitly and interpolates the flow variables at the grid boundaries from the neighboring grids using the interpolation data supplied by the PEGSUS code. The PEGSUS code is used as a preprocessor for the overset grids.

OVERFLOW Navier-Stokes Solver

OVERFLOW is a compressible, thin-layer, Reynolds-averaged Navier-Stokes solver. It accommodates computational domains discretized with overset grids, which are preprocessed with the PEGSUS code. The OVERFLOW code has several discretization and time integration schemes for each subgrid. In this study, for subgrids in which one of the (i, j, k) grid directions aligns with the free-stream flow direction, the partial flux vector splitting algorithm is selected. Otherwise, the 3-factor diagonal scheme with central differencing is employed. The partial flux vector splitting algorithm uses Steger-Warming flux vector splitting for discretization of the convection terms in the stream-wise direction, and central differencing in the other two directions. For the flux splitting algorithm, the central difference smoothing coefficient was gradually reduced to about 0.06 from the starting value of 0.10. For the central difference algorithm on the wing and canard grids the 4^{th} order smoothing coefficient was similarly reduced to 0.08 from 0.1. The flowfield was assumed to be fully turbulent and the Baldwin-Lomax algebraic eddy viscosity model with Degani-Schiff cutoff was employed. Local time stepping was used for convergence to a steady state solution. The convergence criterion was based on the L2 norm of the residuals and the time variation of the integrated aerodynamic loads.

No-slip boundary conditions are applied at the solid surface boundaries. At the farfield boundaries, one-dimensional Riemann invariant extrapolation is employed. At the intergrid boundaries, the flow variables are interpolated from the neighboring grids. The intergrid interpolation stencils and weights are input to the solver. The PEGSUS code is used as a preprocessor to determine the hole boundaries created by the overset grids in the outer grids, and to obtain the intergrid interpolation stencils and the corresponding interpolation weights.

In the OVERFLOW code, the aerodynamic loads are based on the integration of surface pressure and skin friction coefficients. In the present computations, the total aerodynamic loads are obtained by summing up the integrated loads for subgrids with solid surface boundary conditions. It should be noted that this approach does not account for the overlapping grid regions on solid boundaries, which approximately cover less than one percent of the total solid surface area.

Computational Domain

In this study we only considered the flows at 45° roll angle (X-configuration), and zero sideslip angle. The flowfield is therefore assumed to be symmetric with respect to the mid-plane, and only the computational domain over the half-missile configuration is discretized. The computational domain around the canards and the tails, the gaps between the canard and the body, and the zones over the missile body are discretized with structured subgrids. As shown in Figure 2, thirteen subgrids with a total number of approximately 1 million grid points are employed[5]. The canard, tail and gap grids, and the outer grids around them are relatively high resolution viscous grids with clustered grid distributions around the leading edges. The outer boundaries of the computational domain are located about 5 missile lengths away.

RESULTS AND DISCUSSION

We have computed high angle-of-attack, subsonic flowfields over the missile configuration at $\alpha = 15°, 30°, 45°, 60°$ incidences, $M = 0.3$, and $Re_D = 0.95 \cdot 10^6$, where the Reynolds number is based on the diameter of the missile body. Flowfields were assumed to be steady, and the local time-stepping option in the OVERFLOW solver was employed to converge to a stead-state solution. All the computations were carried out on remote CRAY Y-MP and CRAY C90 supercomputers. A typical computation took about 6000-8000 timesteps and 30-40 CPU hours on a CRAY Y-MP.

The FAST flow visualization software from NASA-Ames was utilized for postprocessing the flowfield data. The computed flowfields were analyzed in terms of particle traces, helicity contours and surface streamlines. Helicity is defined as the dot product of velocity and vorticity vectors, which emphasizes the vorticity in the flow direction.

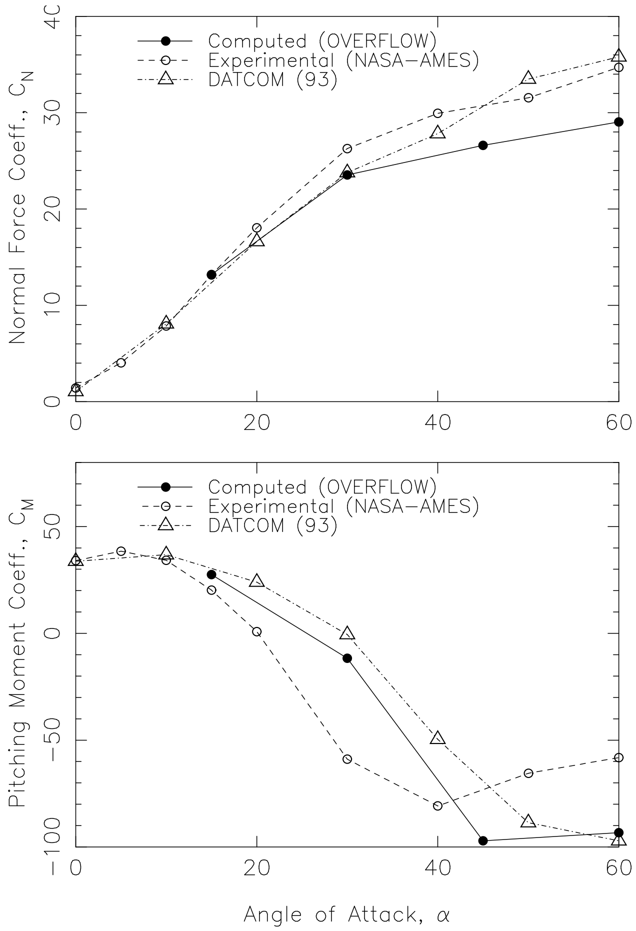

Fig. 3 Aerodynamic loads – $\delta = 10°$, $M = 0.3$, $Re_D = 0.95 \cdot 10^6$

In addition, the integrated aerodynamic loads were compared against the experimental data[9] and the semi-empirical predictions by the missile DATCOM. A series of experiments[9] were performed in the NASA-Ames $7' \times 10'$ Subsonic Wind Tunnel using a 1/3 scale model of the same missile configuration. The model was fitted with boundary layer transition strips at the nose, and the canard and tail fin leading edges. The normal, side and axial forces and pitching, rolling and yawing moments were measured by means of a six-component strain gauge type balance. The tests were performed at $M_\infty = 0.15$

The missile DATCOM is a semi-empirical program originally developed by McDonnell Douglas to calculate the static stability and control characteristics of various missile configurations. It uses analytic methods with experimental data substitution to predict integrated aerodynamic loads.

The computed normal force and pitching moment coefficients are given in Figure 3. The pitching moment convention is positive nose-up and is with respect to the center of gravity, which is located at 11.5 diameters from the missile nose. The reference area is the cross-sectional area of the missile body. Although the normal force is underpredicted and the moment stall is delayed at angles of attack greater than 30°, the computed values agree qualitatively well with the experimental data and the DATCOM predictions. The delay in the predicted pitching moment stall suggests that the loss of suction on the canard surfaces and the missile forebody is underpredicted in the computations. The leveling-off of the moment coefficient at angles of attack greater than 40°, which is captured in the computations, is attributed to the massive flow separation and the stall over the canards, tails and the missile forebody.

Figure 4 shows the flowfield computed at $\alpha = 15°$. As seen in the particle traces and the helicity contours, the flow stays mostly attached over the forebody and the main missile body, except over the canard and tail sections. The leeward side flow over the canards and the tails separates at the leading edges forming leading edge vortices. The leading edge vortices are also depicted by the flow reattachment and the secondary flow separation lines parallel to the leading edges in the surface streamlines. The trajectories and the interaction of the canard vortices are captured in the helicity contours. It is observed that as a result of the interaction the canard vortices roll up in the clockwise direction. It also appears that the upper canard vortex induces a strong downwash on the leeward side of the missile and suppresses the leeward side flow separation behind the canards.

It should be noted that since the gap between the canards and the missile body is modeled, the flow is allowed to pass through the gap as observed in the surface streamlines. However a vortical corner flow still develops below the canard-body junction as observed in the helicity contours. These vortices stay close to the missile body and roll up with the canard vortices as they are convected downstream.

The tail vortices originating from the leading edges of the tails appear to be smaller and weaker than the canard vortices. The separated flow zone at the leeward side of the upper tail is also smaller than that of lower tail and the flow stays mostly attached. This is attributed to the smaller angle of attack the upper tail sees.

At $\alpha = 30°$ the flowfield (Figure 5) is in general similar to that of $\alpha = 15°$, except now the leeward side flow separates at the forebody as well. It is also observed in the helicity contours, which are plotted in the same range, that the leeward side vortices over the missile body are stronger and the recirculating regions grow larger.

The flowfield computed at $\alpha = 45°$ is shown in Figure 6. The flowfield now exhibits a qualitative change: In contrast to the previous cases the coherent leading edge vortices over the lower canard and tail are not observed anymore. On the lower canard, the flow which separates at the leading edge hits the lower surface of the upper canard before it can ever reattach on the upper surface. On the lower tail the reattachment of the flow is not observed either. Instead a corner vortex originating from the apex develops. The separated flow at the leading edge reattaches on the lower surface of the upper tail as shown in the surface streamlines. On the other hand, on the upper canard and tail the leading edge vortices develop and the primary flow reattachment is observed close to the root. The leeward side vortex over the forebody and the missile body, and over the upper tail grow stronger. The flow separation on the leeward side of the forebody also moves closer to the symmetry plane under the influence of the gap flow.

The same flowfield at 45° was also computed by Ekaterinaris[5]. Although the computed flowfields show similar characteristics, the computed normal force and pitching moment coefficients are given in Reference 5 as 32.7 and -71.9, respectively, in contrast to 26.6 and -97.1 in the present computations. Further work is necessary to identify the precise reasons for this discrepancy.

Figure 7 shows the flowfield computed at $\alpha = 60°$. Besides the larger recirculation regions on the leeward side of the missile body, the flowfield shows similar characteristics to the one at $\alpha = 45°$.

CONCLUDING REMARKS

A thin layer Navier-Stokes solver with overset grids, OVERFLOW, was employed to compute the subsonic flowfields over a missile configuration at high angles of attack ranging from 15° to 60°. The canard and tail vortices, their interaction, and the flow separation over the missile body are identified. The computed normal force and pitching moment coefficients agree well with the measurements at 15° angle of attack, but the normal force predictions deviate by up to 15 percent at the higher incidences. The pitching moment predictions show larger percentage deviations from the experiment at the higher angles of attack. However, the qualitative trends are correctly predicted, showing improvement over the DATCOM predictions. Further computations are needed to explore the asymmetric vortex shedding, the grid sensitivity, the effect of higher order turbulence models and the inclusion of boundary layer transition models. Also, detailed flowfield measurements are needed for an ultimate assessment of the computational accuracy rather than comparisons with total force and moment measurements.

Although the computations are CPU intensive and convergence for separated flows is slow, the OVERFLOW Navier-Stokes solver with overset grids is an effective tool in the analysis of separated, vortical flowfields over full missile configurations.

ACKNOWLEDGMENT

The authors are grateful to Dr. J.A. Ekaterinaris for providing the computational grid. Also, they wish to thank Mr. David Siegel, Office of Naval Research, and Dr. Craig Porter and Mr. C. Housh, Naval Air Warface Center Weapons Division, China Lake, for their support of this project. This work was supported in part by a grant of HPC time from the DoD HPC Centers Vicksburg (CRAY Y-MP) and Stennis (CRAY C90).

REFERENCES

1. Rom, J. *High Angle of Attack Aerodynamics*, ISBN 0-387-97672-8, Springer-Verlag New York, 1992.

2. *Tactical Missile Aerodynamics,* edited by Hemsch, M.J. and Nielsen, J.N., ISBN 0-930403-13-4, AIAA, New York, 1986.

3. Degani, D. and Schiff, L.B., *Computation of Turbulent Supersonic Flows around Pointed Bodies Having Crossflow Separation,* Journal of Computational Physics, Vol. 66, No. 1, 1986, pp. 173-196.

4. Schiff, L.B., Degani, D. and Gavali, S., *Numerical Simulation of Vortex Unsteadiness on Slender Bodies of Revolution at Large Incidence,* AIAA paper 89-0195, 1989.

5. Ekaterinaris, J.A. *Analysis of Flowfields over Missile Configurations at Subsonic Speeds,* Journal of Spacecraft and Rockets, volume 32, Number 3, pp. 385-391, May-June 1995.

6. Hsieh, T., Priolo, F.J., and Wardlaw, A.B.Jr., *Navier-Stokes Calculation of Flow Over a Complete Missile to 60 Degree Incidence,* AIAA paper 95-0760, 1995.

7. Tuncer, I.H., Marvin, R. and Platzer M.F., *Numerical Investigation of Subsonic Flow over a Typical Missile Forebody,* AIAA paper 96–0189, 34^{th} AIAA Aerospace Sciences Meeting and Exhibit, Reno, NV, January 15-18, 1996.

8. Smith, E.H., Hebbar S.K., and Platzer, M.F., *Aerodynamic Characteristics of a Canard-Controlled Missile at High Angles of Attack,* Journal of Spacecraft and Rockets, Volume 31, Number 5, pp. 766-772, Sep-Oct 1994.

9. Smith, B.E. and Smith, E.H., *High Angle-of-Attack Wind Tunnel Test in NASA AMES 7-by10 Foot Wind Tunnel*, Unpublished Data Report, August 1992

10. Ying, S.X., Steger, J.L., Schiff, L.B. and Baganoff, D. *Numerical Simulation of Unsteady, Viscous High-Angle-of-Attack Flows Using a Partially Flux-Split Algorithm,* AIAA Paper 86-2179, 1986

11. Benek, J.A., Buning, P.G., and Steger, J.L., *A 3D Chimera Grid Embedding Technique,* AIAA Paper 85-1523, July 1985.

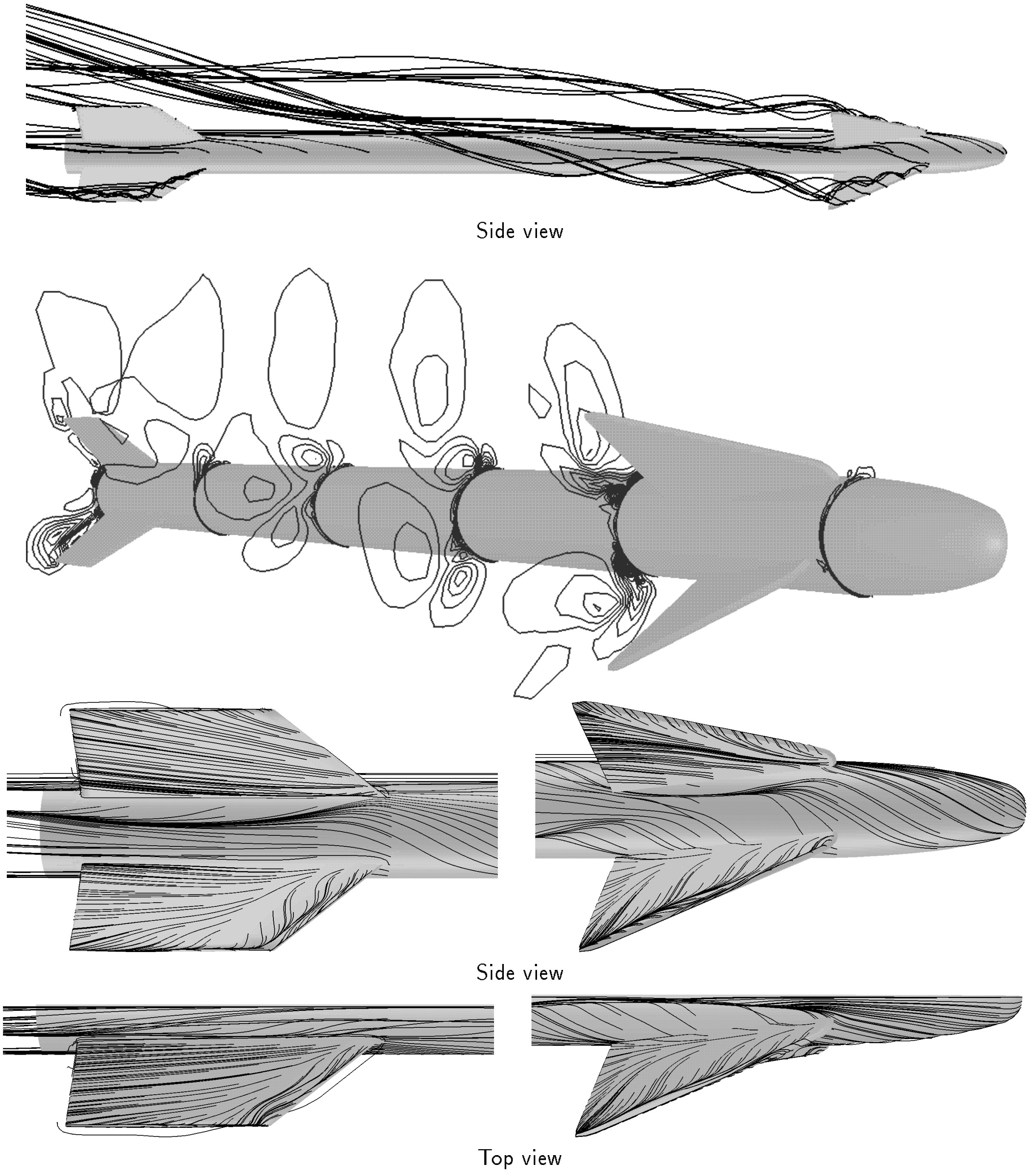

Fig. 4 Particle traces, helicity contours and surface streamlines at the forebody and tail sections at $\alpha = 15°$, $\delta = 10°$, $M = 0.3$, $Re_D = 0.95 \cdot 10^6$

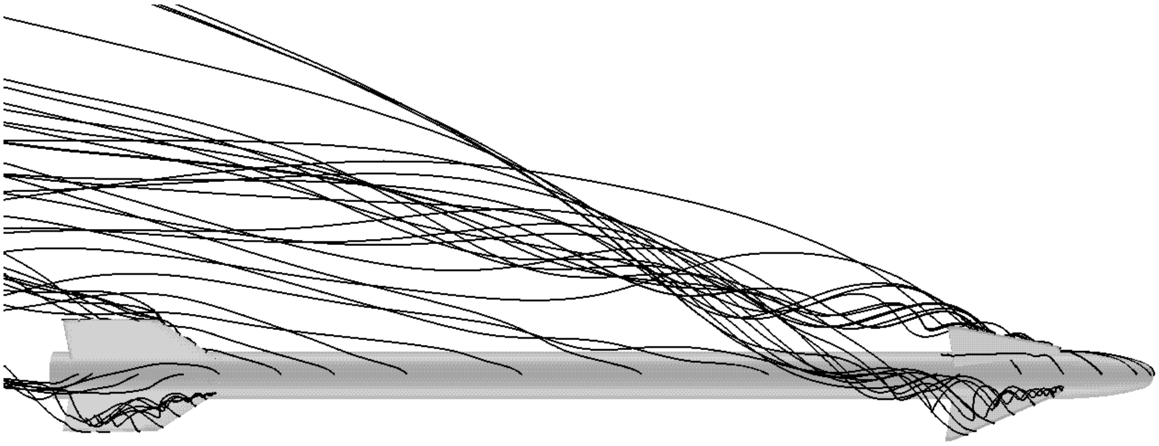

Side view

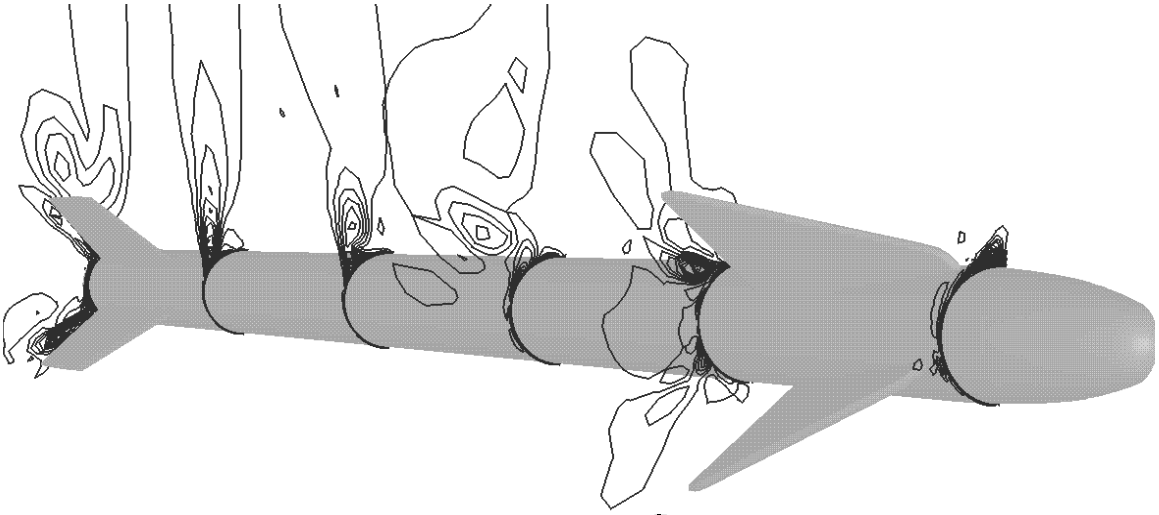

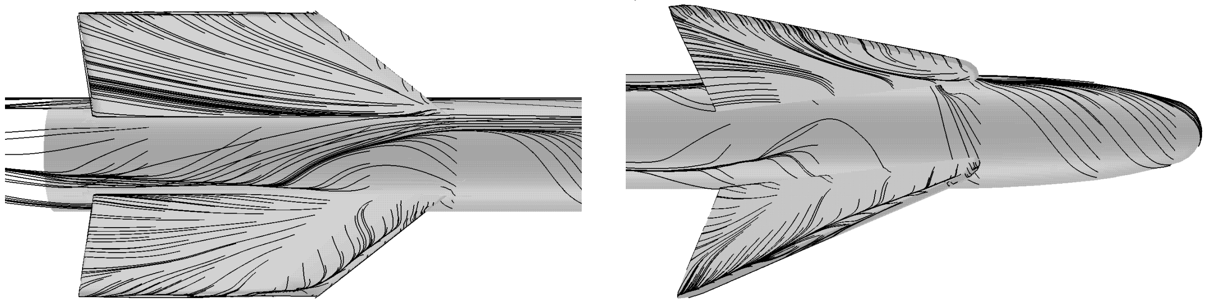

Side view

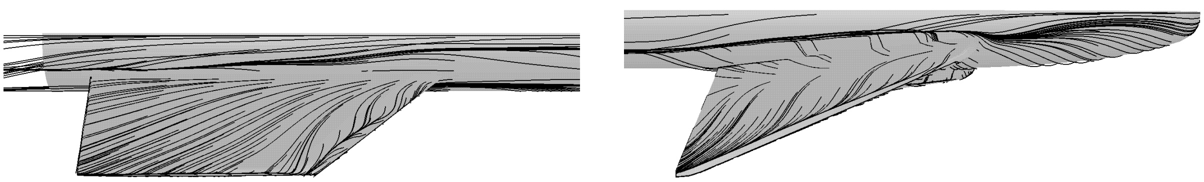

Top view

Fig. 5 Particle traces, helicity contours and surface streamlines at the forebody and tail sections at $\alpha = 30°$, $\delta = 10°$, $M = 0.3$, $Re_D = 0.95 \cdot 10^6$

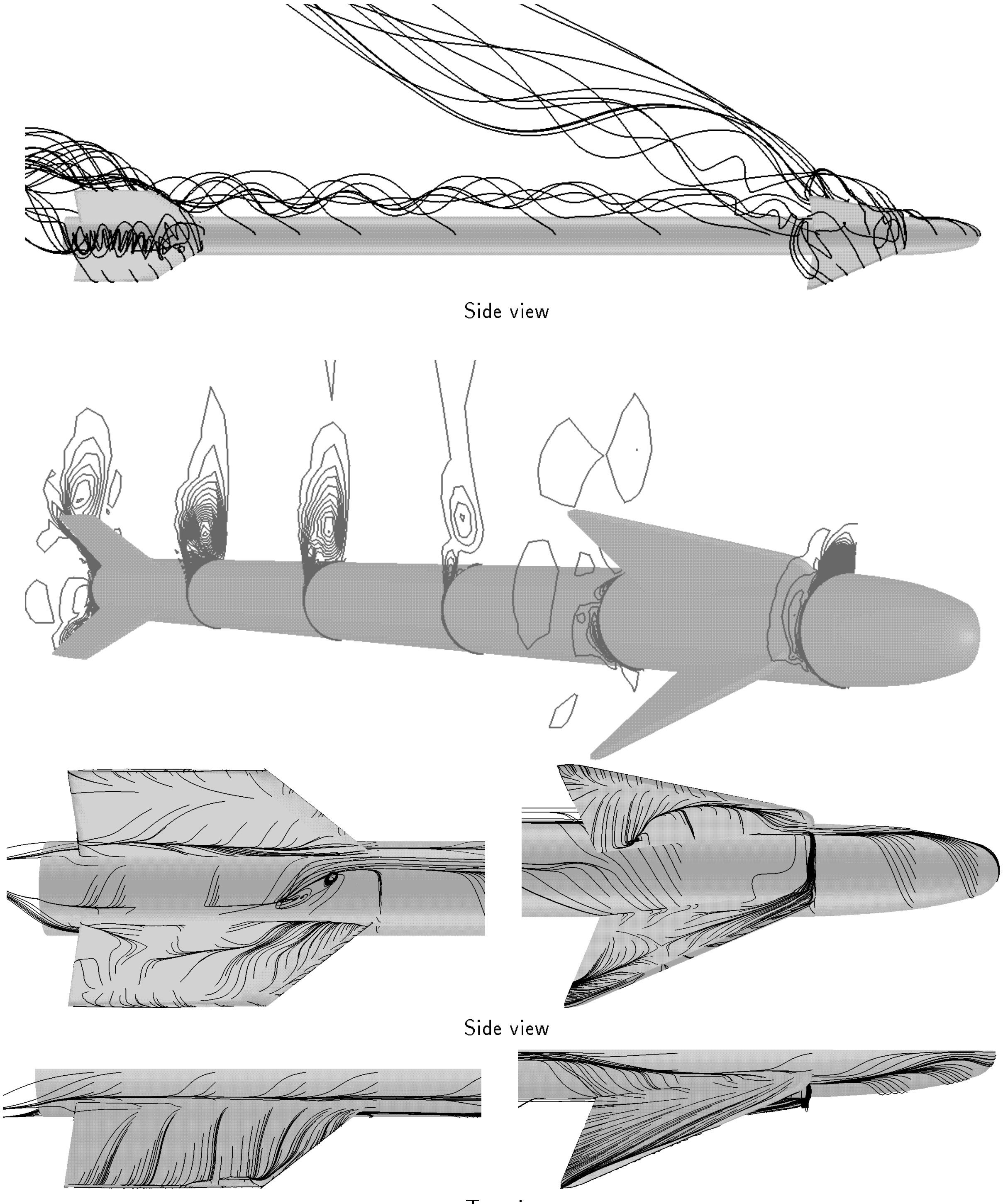

Fig. 6 Particle traces, helicity contours and surface streamlines at the forebody and tail sections at $\alpha = 45°$, $\delta = 10°$, $M = 0.3$, $Re_D = 0.95 \cdot 10^6$

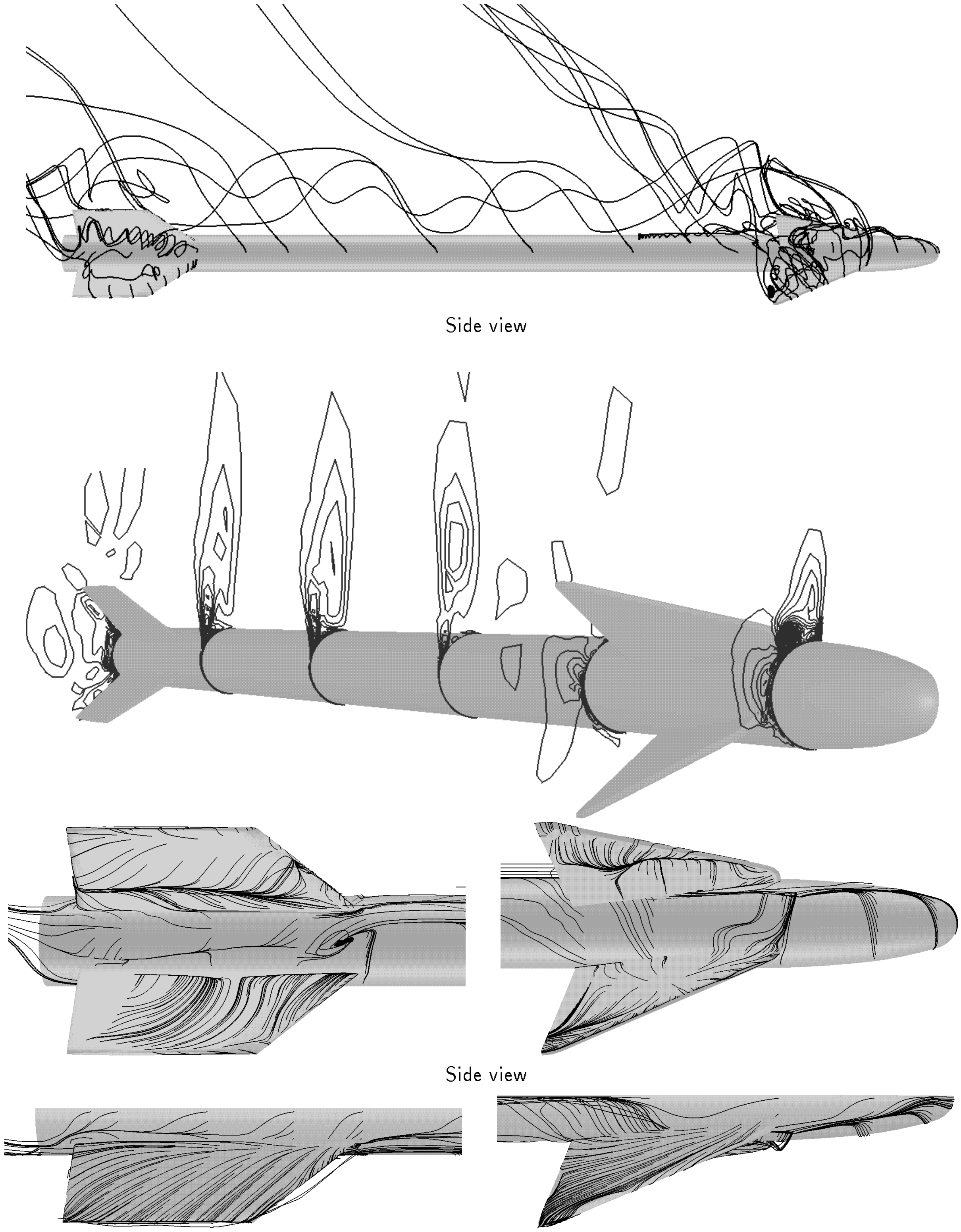

Fig. 7 Particle traces, helicity contours and surface streamlines at the forebody and tail sections at $\alpha = 60°$, $\delta = 10°$, $M = 0.3$, $Re_D = 0.95 \cdot 10^6$